ELSEVIER

Journal of Hydrology 244 (2001) 43–59

Journal of Hydrology

www.elsevier.com/locate/jhydrol

Comparison of uncertainty analysis methods for a distributed rainfall–runoff model

Pao-Shan Yu[a,*], Tao-Chang Yang[b], Shen-Jan Chen[b]

[a]*Department of Hydraulics and Ocean Engineering, National Cheng Kung University, Tainan 70101, Taiwan, ROC*
[b]*Tainan Hydraulics Laboratory, National Cheng Kung University, Tainan 70101, Taiwan, ROC*

Received 10 May 2000; revised 25 August 2000; accepted 21 December 2000

Abstract

A rainfall–runoff model is normally applied to storm events outside of the range of conditions in which it has been successfully calibrated and verified. This investigation examined the uncertainty of model output caused by model calibration parameters. Four methods, the Monte Carlo simulation (MCS), Latin hypercube simulation (LHS), Rosenblueth's point estimation method (RPEM), and Harr's point estimation method (HPEM), were utilized to build uncertainty bounds on an estimated hydrograph. Comparing these four methods indicates that LHS produces analytical results similar to those of MCS. According to our results, the LHS only needs 10% of the number of MCS parameters to achieve similar performance. However, the analysis results from RPEM and HPEM differ markedly from those from MCS due to the very small number of model parameters.

Keywords: Monte Carlo; Latin hypercube; Harr's point estimation method; Rosenblueth's point estimation method; Rainfall–runoff model; Uncertainty analysis

1. Introduction

Rainfall–runoff models are generally required to forecast operational floods and perform the design-flood estimation of synthetic flows in water resource projects. Strong interest in the application of rainfall–runoff models to water resource projects demands increasing attention to further developing distributed rainfall–runoff models and model reliability analysis. Distributed rainfall–runoff models, capable of simulating the heterogeneity of both rainfall spatial distribution and catchment characteristics, are a highly promising alternative for simulating flood hydrographs. Moreover, potential applications of physical-based distributed models include forecasting the effects of land-use change, the effects of spatially variable inputs and outputs, the movement of pollutants and sediments and the hydrological response of ungauged catchments where no data are available for calibrating lumped models (Beven and O'Connell, 1982). Hence, numerous distributed rainfall–runoff models have been proposed to simulate flood hydrographs more accurately (Jønch-Clausen, 1979; Abbott et al., 1986; Morris, 1980; Edward et al., 1977; Ross et al., 1979; Jayawardena and White, 1977, 1979; Laurenson, 1964; Diskin and Simpson, 1978; Diskin et al., 1984; Knudsen et al., 1986; Beven et al., 1984).

Increasing attention has been paid to accurately predict the model reliability when applying the models to storms and watershed conditions beyond

* Corresponding author. Fax: +886-6-274-1463.
E-mail addresses: yups@mail.ncku.edu.tw (P.-S. Yu), tcyang@mail.ncku.edu.tw (T.-C. Yang).

0022-1694/01/$ - see front matter
PII: S0022-1694(01)00328-6

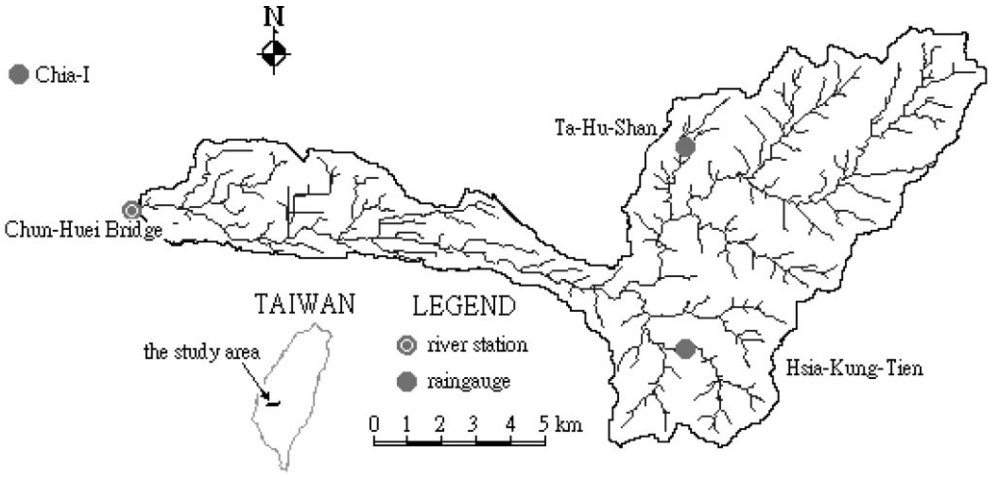

Fig. 1. The channel networks upstream the study area.

the range of conditions for which the model has been successfully calibrated and verified. In a related investigation, Beven (1989) recommended that a realistic estimate of prediction uncertainty is required owing to the limitation of generating the currency of distributed physically based rainfall–runoff models. Melching (1995) reviewed relevant literature on various reliability analysis methods of rainfall–runoff models including the Monte Carlo simulation method (MCS) (Binley et al., 1991; Beven and Binley, 1992), Latin hypercube simulation method (LHS) (Melching, 1992a,b), MFOSM, AFOSM and Rosenbruth's point estimation method (RPEM) and Harr's point estimation method (HPEM).

Table 1
Historical storm events for this study

Storm event	Date of occurrence	Peak discharge ($m^3 s^{-1}$)	Rainfall duration (h)	Rainfall depth (mm)	Calibration or verification[a]
I	1982.7.29	711	40	310.06	C
II	1988.8.13	799	40	410.68	C
III	1989.7.27	521	24	217.49	C
IV	1991.6.22	235	72	337.29	C
V	1991.7.28	550	24	176.59	C
VI	1992.8.30	966	48	588.61	C
VII	1981.7.22	366	72	306.34	V
VIII	1986.8.22	734	24	241.87	V
IX	1987.7.27	847	48	485.69	V

[a] "C" means calibration and "V" means verification.

Many previous investigations have compared the relative performances of various reliability analysis methods (Melching, 1992a,b; Bates and Townley, 1988; Lei and Schlling, 1993; Garen and Burges, 1981; Binley et al., 1991). Melching (1995) recommended more closely examining the feasibility of applying HPEM and LHS methods to rainfall–runoff models.

In light of the above discussion, this work investigates the feasibility of applying various methods of uncertainty analysis to a distributed rainfall–runoff model including MCS, LHS, RPEM and HPEM. The study attempts to simulate the hydrographs and their uncertainty bounds for a catchment with limited historical storm records. A grid-square based distributed rainfall–runoff model (Yu and Liu, 1992; Yu and Zheng, 1997) is selected to take into consideration the spatial variability of catchment characteristics. Hence the catchment is divided into 1 km by 1 km grid-based meshes. Each grid is treated as a conceptual linear reservoir in which a time lag is considered and hydrological processes simulated to ensure that the model is not too costly to run. Furthermore, the global optimization technique is applied to ensure that the calibrated parameters are optimal.

2. Study area

The upstream catchment of Pa-Chang Creek, chosen as the study area, is located in southern Taiwan

(Fig. 1). The catchment has an area of 122 km^2 and the mainstream length is approximately 32 km. The Chun-Huei Bridge is the outlet of the study area. Flood and inundation frequently occur in the downstream area of Pa-Chang Creek owing to the abundant precipitation in the upstream catchment as well as the mild slope and meandering of the middle and downstream reaches of Pa-Chang Creek.

Nine of the larger storm events were collected as listed in Table 1. Six of these events were arbitrarily chosen to calibrate the model while the others were used to verify the model. Three recording rain gauges provide hourly rainfall data in this work. The soil types in this area largely belong to sandy loam, loam or silty loam. The ground cover is primarily forest and betel nut upstream of the catchment. The main vegetation downstream are rice paddies and orchards.

3. Distributed rainfall–runoff model

The distributed rainfall–runoff model developed for the studied catchment includes three basic elements: simulation of catchment characteristics, abstraction loss, and basic flow equations.

3.1. Catchment characteristics

The distributed model divides a catchment into a 1×1 km^2 grid-based mesh. To abstract the geometry of the catchment characteristics, topography and channel configuration are modeled on this scale from soil, land use, and topography maps.

As the rainfall data derived from radar has not yet been applied in Taiwan for hydrological applications, the data from three recording rain gauges are employed as input data. To consider the spatial distribution of rainfall, the Thiessen method is used to determine the control area for each rain gauge.

3.2. Abstraction loss

Some of the rainfall is lost due to evaporation, interception, and infiltration before being converted into runoff. Since only net rainfall contributes to runoff, the rainfall–runoff models must simulate the separation of net rainfall. Notably, only infiltration loss is considered here because infiltration is always assumed to dominate the abstraction losses. The Horton infiltration equation (Waren et al., 1989) is

$$f_p(t) = f_c + (f_0 - f_c)\, e^{-kt} \tag{1}$$

where $f_p(t)$ denotes the infiltration capacity, f_c represents the initial infiltration capacity, f_0 is the final infiltration capacity, k denotes the decay constant, and t is the time.

Eq. (1) implies that the infiltration capacity is the only function of time and is always decreasing with time even if the rainfall stops or becomes relatively smaller than the infiltration capacity. In reality, the infiltration rate at any time is equal to the minimum of the infiltration capacity $f_p(t)$ or rainfall intensity $i(t)$. Hence, the actual infiltration can be expressed as

$$f(t) = \min[f_p(t), i(t)] \tag{2}$$

To adjust for this deficiency, the integrated form of Horton's equation is used:

$$F(t_p) = \int_0^{t_p} f_p(t)\, dt = f_c t_p + \frac{f_0 - f_c}{k}(1 - e^{-kt_p}) \tag{3}$$

where t_p represents the equivalent time for the actual infiltration volume to equal the infiltration volume estimated by Horton's equation.

Following modification by the equivalent time t_p, the Horton's infiltration equation can be employed directly to estimate the infiltration. Based on the soil maps (The Council of Agriculture of ROC, 1988), the parameters f_0, f_c, and f_k can be determined. Additionally, the antecedent condition significantly influences the value of initial infiltration capacity f_0. Therefore, a factor (CH) is used to adjust the value of f_0 to each storm event:

$$(f_{0,opt})_i = CH(f_{0,doc})_i \tag{4}$$

where $(f_{0,opt})$ is the optimal initial infiltration capacity at the ith grid element and $(f_{0,doc})$ is the value of f_0 for the ith grid element chosen via documentary data based on the soil type.

The antecedent condition normally influences the initial infiltration capacity f_0 to such an extent that the value of $(f_{0,doc})$ from document ranges widely. Herein, its average value is chosen as $(f_{0,doc})$ in the work. As generally known, each storm event has its own antecedent condition and optimal initial infiltration

Table 2
The optimal parameter sets for six calibration storm events and the range of each parameter for uncertainty analysis

Storm event	K_s (min)	K_c (min)	*CH*	$\Delta Q_p/Q_p$ (%)	ΔT_p (h)	OBJ
I	52.0	0.80	0.40	20.11	1	114.22
II	50.0	0.42	2.07	8.26	0	106.47
III	50.0	1.00	1.75	10.75	1	75.98
IV	50.0	4.00	0.69	−10.26	1	38.51
V	44.0	1.92	0.80	−5.82	0	25.27
VI	50.0	5.00	0.03	7.97	−4	113.41
Range of parameter	44.0–52.0	0.42–5.00	0.03–2.07			
Mean value	49.33	2.19	0.96			
Standard deviation	2.73	1.88	0.79			

capacity, which explains why this work uses a calibrated parameter *CH* to obtain the optimal initial infiltration parameter. The spatial variability of infiltration parameter over each grid element can be still reserved in terms of ($f_{0,doc}$) although a lumped parameter *CH* is used and calibrated.

3.3. Flow governing equations

In the distributed model, the linear conceptual approaches are employed separately for overland flow and channel flow routing. The catchment storage effects are represented by the linear storage element (Pederson et al., 1980). The basic equations are as follows:

Continuity equation:

$$I - Q = \mathrm{d}S/\mathrm{d}t \tag{5}$$

Storage equation:

$$S = KQ \tag{6}$$

where I is the inflow, Q represents outflow, S is storage, and K denotes storage coefficient. Actually, two parameters K_s and K_c, namely the storage coefficients in the overland flow and channel flow, respectively, are used in the model and calibrated by using historical storm events.

To solve Eqs. (5) and (6), the governing equation in linear model is written as

$$Q_{t+1} = \frac{2K - \Delta t}{2K + \Delta t} Q_t + \frac{\Delta t}{2K + \Delta t}(I_{t+1} + I_t) \tag{7}$$

4. Model calibration

This study divides the model parameters of the distributed rainfall–runoff model into two kinds: model input parameters (i.e. input data), which can be read directly from topographic, soil, and vegetation maps, and model calibration parameters, which are calibrated from historical rainfall and flow data. Three calibration parameters (namely, K_S, K_C, and *CH*) in the model must be calibrated by applying the optimization technique. Many researchers have conferred that global optimization techniques can overcome the presence of multi-local and discontinuous derivatives (Sorooshian et al., 1993; Brazil and Krajewski, 1987). Among global optimization techniques, the shuffled complex evolution (SCE) method is a highly effective means of calibrating a model as confirmed by Sorooshian et al. (1993). Details of the SCE method are reported in the studies of Duan et al. (1992, 1993). Hence, this study adopts the SCE method to calibrate the model.

Six historical storm events and another three historical storm events in the period from 1981 to 1991 (listed in Table 1) are arbitrary selected to calibrate and verify the model, respectively. The hourly rainfall data are provided by three recording rain gauges. The infiltration parameters f_0, f_c, and f_k are determined based on the maps of land use and soil type for each grid to display the spatial variability of infiltration. This work assumes that the ground cover essentially remains unchanged from 1981 to 1992 during which period the historical storm events are collected for model calibration and verification. Calibration results in Table 2 indicate that the error ratio of the estimated

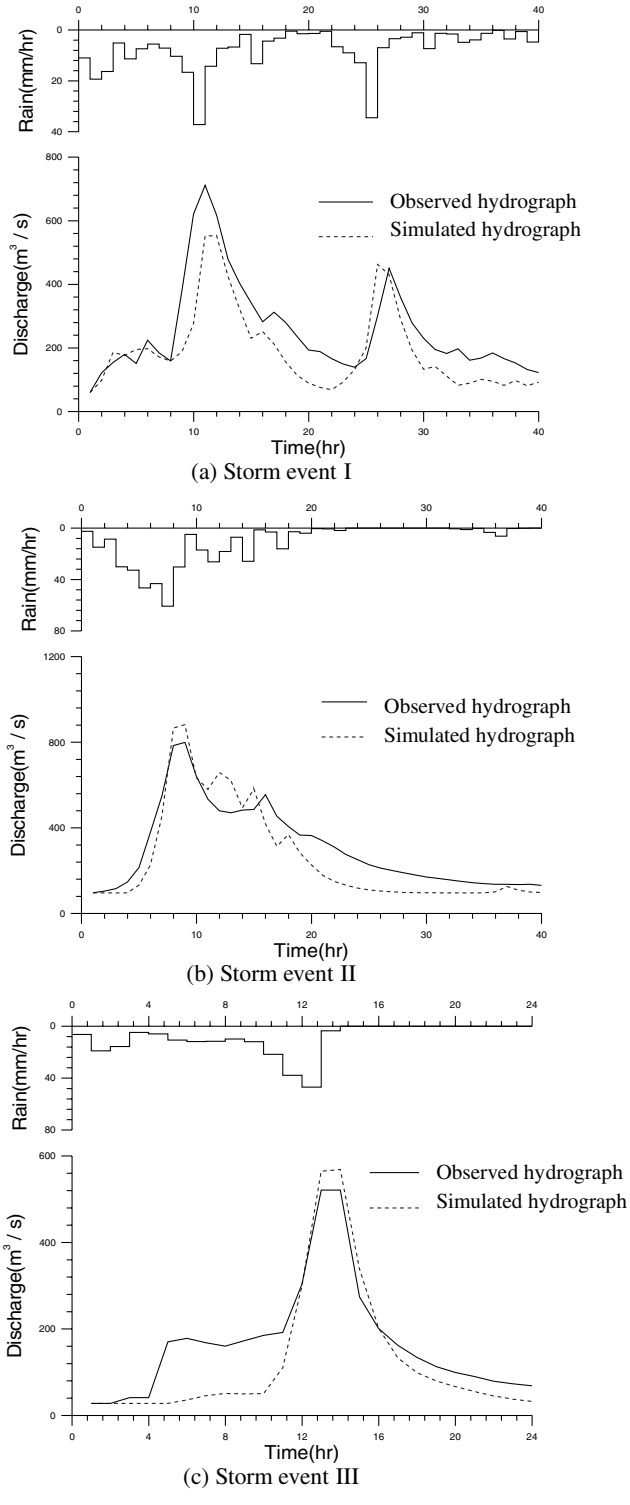

Fig. 2. The calibration results of storm events I, II, and III, respectively.

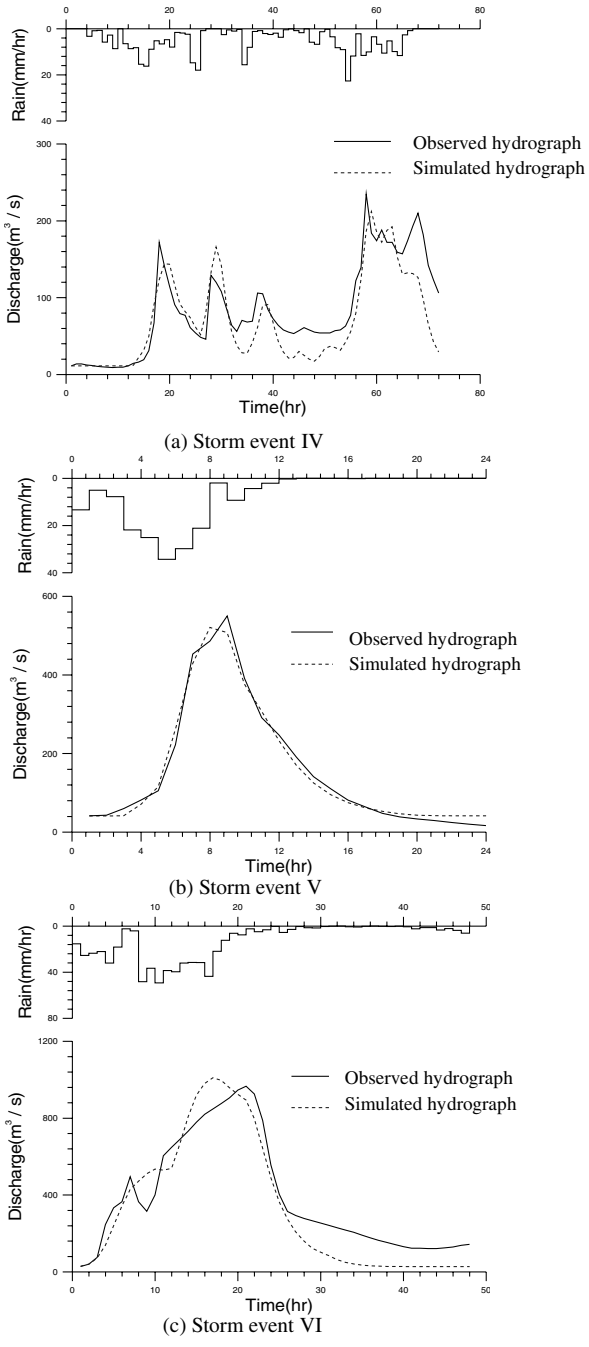

Fig. 3. The calibration results of storm events IV, V, and VI, respectively.

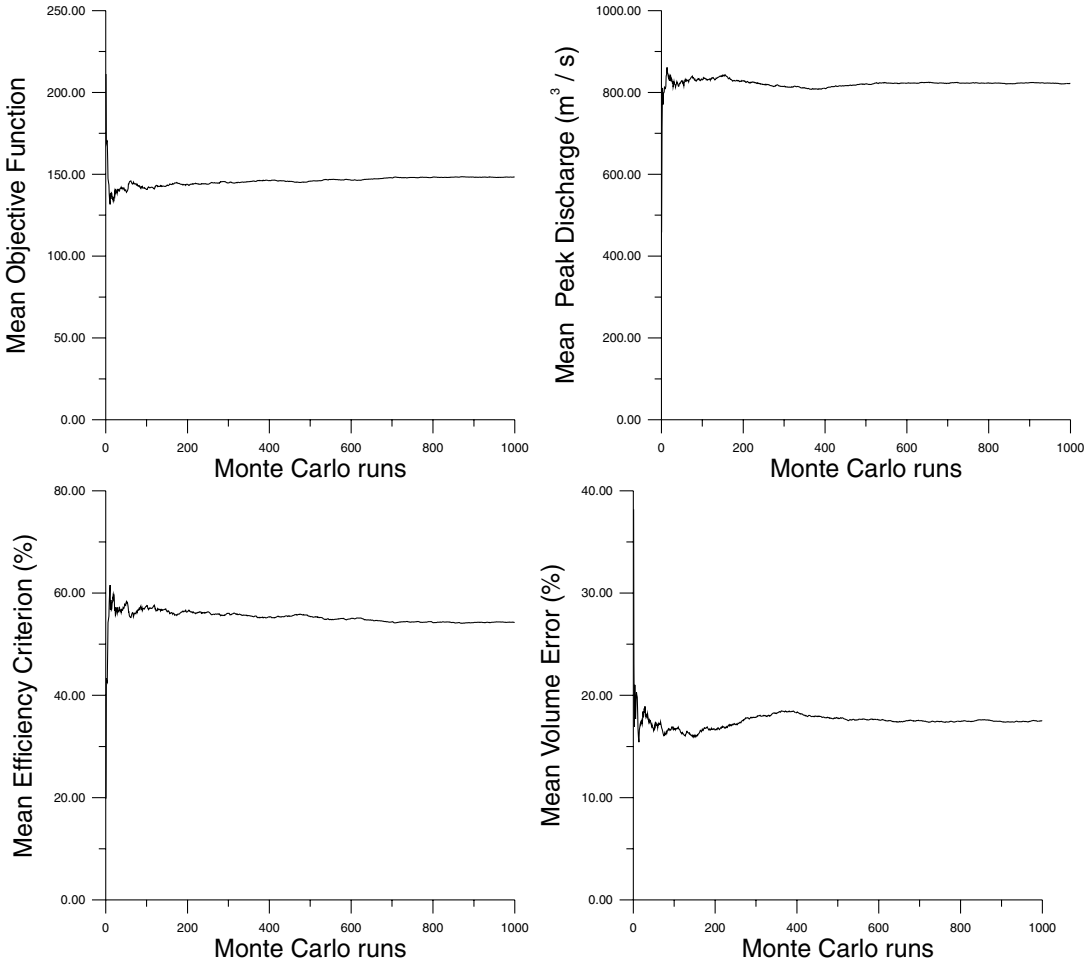

Fig. 4. The mean values of output statistics estimated by the MCS for various runs.

peak flow (ΔQ_p) to the observed peak flow (Q_p) for each storm event is reasonable. Most calibration storm events have a peak error of below 11%. Additionally, the error of time to peak (ΔT_p) is small for every storm event except storm event IV. Figs. 2 and 3 display the estimated and observed hydrographs for all calibration storm events revealing that the model can simulate the historical rainfall–runoff relationship.

5. Method of uncertainty analysis

Melching (1995) thoroughly reviewed various methods of uncertainty analysis on rainfall–runoff models. The methods are briefly described in the following sections.

5.1. Monte Carlo simulation

Various methods have been applied to obtain output reliability given the range of model parameters. MCS is commonly selected as a standard means of comparison against other methods. MCS generates a large number of realizations of model parameters according to their corresponding probability distribution.

The uniform distributions with lower and upper bounds are assumed to present the variation of calibrated parameters (i.e. K_S, K_C, and CH). The

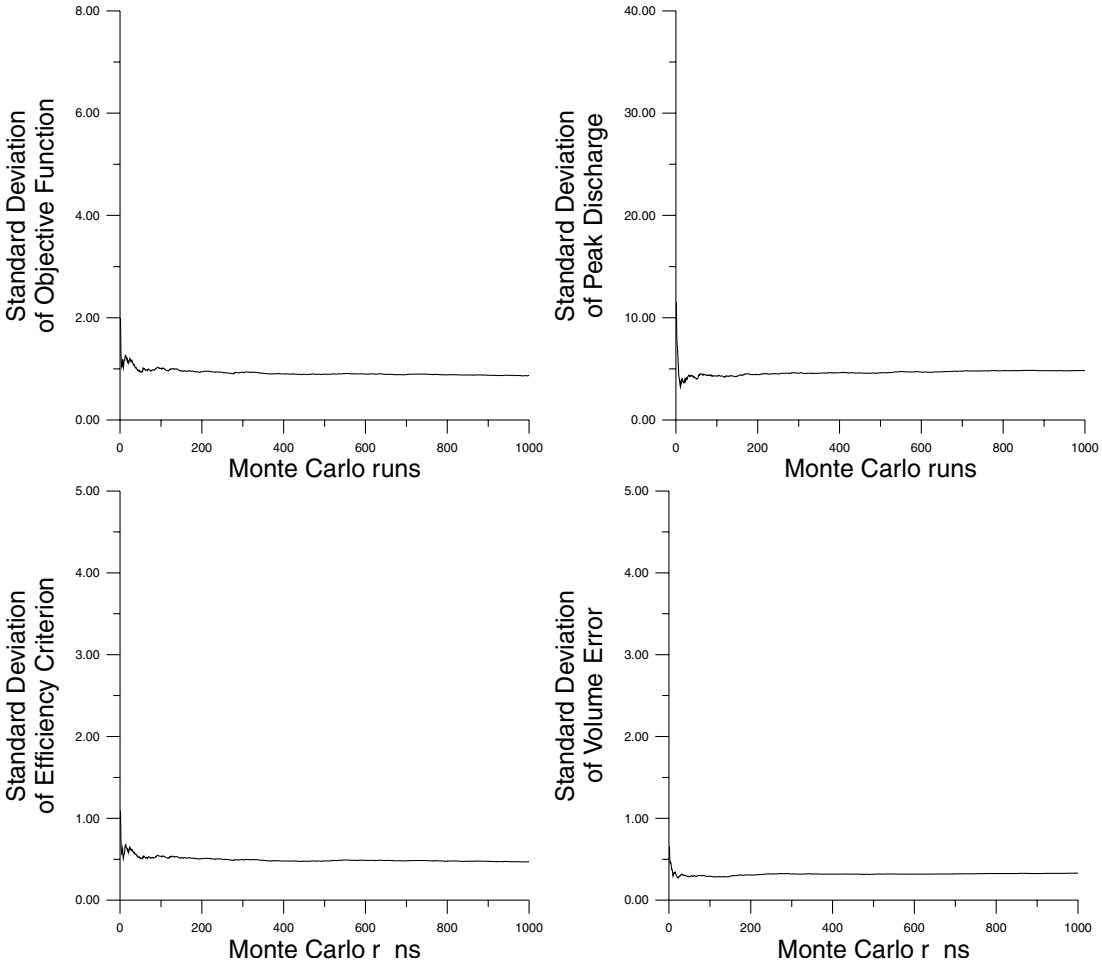

Fig. 5. The standard deviations of output statistics estimated by the MCS for various runs.

maximum and minimum values of each parameter in Table 2 are chosen as the lower and upper bounds. To find how many realizations were sufficient to analyze the uncertainty of model output, the values of mean and standard deviation of the output statistics (mean model efficiency, mean volume error, mean peak flow and mean objective function) were calculated and plotted after each realization. Figs. 4 and 5 illustrate the values of mean and standard deviations for the above four criteria, respectively, for storm event VIII. Both figures reveal that both mean and standard deviations of model output statistics from 1000 realizations converge to constant values, respectively. The same results were observed in the other storm events.

Therefore, 1000 runs were randomly generated for each parameter, producing 1000 parameter sets. The distributed rainfall–runoff model was implemented with these generated parameter sets to simulate 1000 hydrographs by which values of mean and standard deviation of discharge at each time instant were further calculated. The uncertainty bounds of simulated hydrograph can be presented by indicating mean $\pm 2 \times$ standard deviations at each time step.

5.2. Latin hypercube simulation

LHS is a stratified sampling approach that efficiently estimates the statistics of an output. The probability distribution of each basic variable is subdivided into N ranges with an equal probability

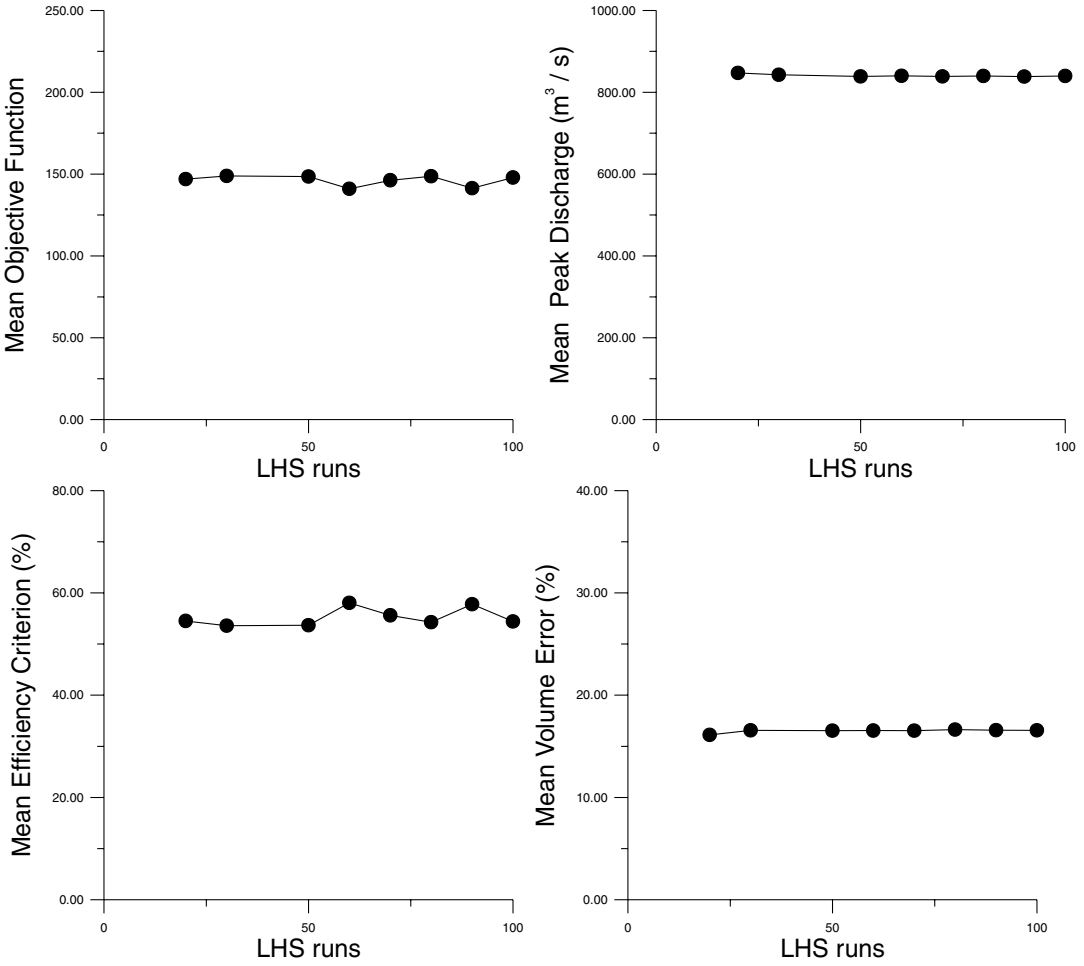

Fig. 6. The mean values of output statistics estimated by the LHS for various runs.

of occurrence (1/*N*). Random values of the basic variable are simulated such that each range is sampled just once. The order of selection the ranges is randomized and the model is executed *N* times with a random combination of basic variable values from each range for each basic variable.

As an example for storm event VIII, Figs. 6 and 7 illustrate the values of the mean and standard deviation of model output statistics for various numbers of *N*, respectively. According to these figures, both the mean and standard deviations of model output statistics converge to constant values when *N* equals 100. The same results were observed when using other storm events.

Therefore, $N = 100$ is sufficient for the LHS in the investigation. One hundred runs were randomly generated for each parameter (i.e. K_S, K_C, and *CH*) and 100 parameter sets could be captured. Using these generated parameter sets, 100 hydrographs were simulated for a storm event by using the distributed rainfall–runoff model. Values of mean and standard deviation of discharge at each time instant were then calculated by using these 100 simulated hydrographs to display the uncertainty bounds by indicating mean $\pm$ 2 $\times$ standard deviations.

5.3. Rosenblueth's point estimation method

The point estimation method was originally proposed by Rosenblueth (1975) to deal with symmetric, correlated, and stochastic input parameters. The method

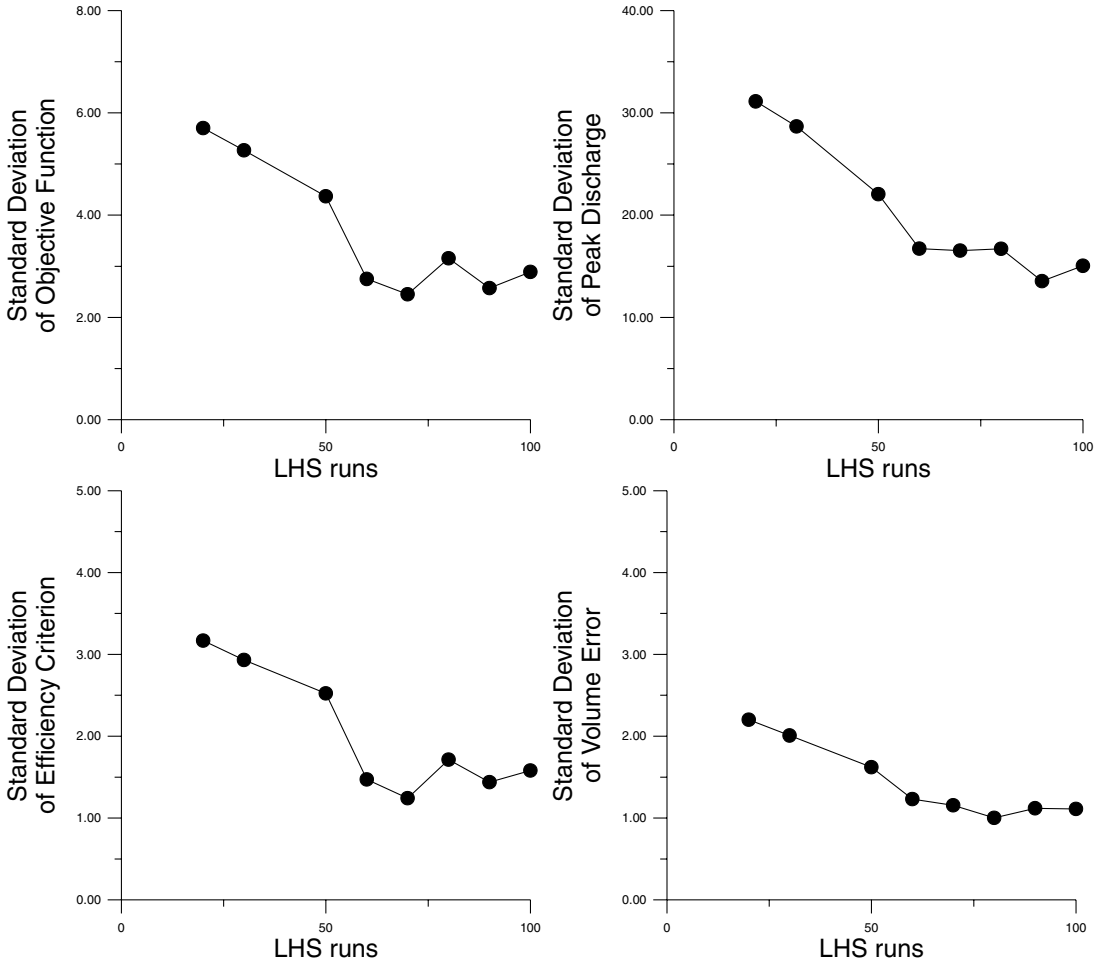

Fig. 7. The standard deviations of output statistics estimated by the LHS for various runs.

was later extended to the case involving asymmetric random variable. The idea is to approximate the original probability density function (PDF) of a random variable by discrete probability masses concentrated at two points in such a way that the first three moments of the original PDF are preserved. In RPEM (Rosenblueth 1975, 1981), the Nth moment of Q around the origin (i.e. $E[Q^N]$) can be approximated via a point-probability estimate of the first-order Taylor series expansion as

$$E[Q^N] \approx [(q_{+++\ldots p})(Q_{+++\ldots p})^N + (q_{-++\ldots p}) \times (Q_{-++\ldots p})^N + \cdots + (q_{---\ldots p})(Q_{---\ldots p})^N] \quad (8)$$

where

$$Q_{+++\ldots p} = H(x_1 + \sigma_1, x_2 + \sigma_2, \ldots, x_p + \sigma_p), \quad (9)$$

$$Q_{---\ldots p} = H(x_1 - \sigma_1, x_2 - \sigma_2, \ldots, x_p - \sigma_p). \quad (10)$$

The various other + and − subscripts for Q refer to the mean of basic variable x_i plus or minus, respectively, one standard deviation σ_i and H represents a function representing the output of distributed rainfall–runoff model in this study. Meanwhile, the weighting function of q is

expressed as

$$q_{ijk\ldots p} = \frac{\left(1 + \sum_{g=1}^{p}\sum_{h=1}^{p} g'h'\partial_{g,h}\rho_{g,h}\right)}{2^p} \quad (11)$$

where $\partial_{g,h}$ is 0 if $g \geq h$, $\partial_{g,h}$ is 1 if $g < h$, $\rho_{g,k}$ is the correlation coefficient of random variables x_g and x_h, and g' and h' are -1 or $+1$ depending on the sign of the q function subscript for the basic variable being considered. As an illustration, the eight weighting functions for a function of three random variables ($p = 3$) are as follows:

$$q_{+++} = q_{---} = (1 + \rho_{12} + \rho_{13} + \rho_{23})/2^3 \quad (12)$$

$$q_{++-} = q_{--+} = (1 + \rho_{12} - \rho_{13} - \rho_{23})/2^3 \quad (13)$$

$$q_{-+-} = q_{+-+} = (1 - \rho_{12} - \rho_{13} + \rho_{23})/2^3 \quad (14)$$

$$q_{+--} = q_{-++} = (1 - \rho_{12} + \rho_{13} - \rho_{23})/2^3 \quad (15)$$

Using this method to estimate the uncertainty of simulated hydrograph, the values of mean and standard deviation of each parameter (i.e. K_S, K_C, and CH) were first calculated (Table 2) from the calibrated values of the six calibrated storm events. The correlation matrix of parameters, K_S, K_C, and CH, is estimated as

$$\rho = \begin{bmatrix} 1 & -0.045 & -0.016 \\ -0.045 & 1 & -0.70 \\ -0.016 & -0.70 & 1 \end{bmatrix}$$

where K_{S+} and K_{S-} represent the mean of K_S plus and minus, respectively, one standard deviation, as follows:

$$K_{S+} = 49.33 + 2.73 = 52.06$$

$$K_{S-} = 49.33 - 2.73 = 46.60$$

where K_{C+}, K_{C-}, CH_+, and CH_- were calculated in the same way and have values of 4.07, 0.31, 1.75, and 0.17, respectively.

Eight sets of parameters (i.e. [K_{S+}, K_{C+}, CH_+], [K_{S-}, K_{C-}, CH_-], [K_{S+}, K_{C+}, CH_-], [K_{S-}, K_{C-}, CH_+], [K_{S+}, K_{C-}, CH_+], [K_{S-}, K_{C+}, CH_-], [K_{S+}, K_{C-}, CH_-], and [K_{S-}, K_{C+}, CH_+]) can be obtained by arranging K_{S+}, K_{C+}, CH_+, K_{S-}, K_{C-}, and CH_-. Eight hydrographs (i.e. model output H) were simulated using these eight sets of parameters. The values of the eight weighting functions calculated by using Eq. (11) are $q_{+++} = q_{---} = 0.030$, $q_{++-} = q_{--+}0.208$, $q_{+-+} = q_{-+-} = 0.216$, and $q_{+--} = q_{-++} = 0.046$. The expected value of model output $E(Q)$ can be estimated using Eq. (8) and the variance of model output Var(Q) can be obtained with the following equation:

$$\mathrm{Var}(Q) = E[Q^2] - E^2[Q] \quad (16)$$

The uncertainty bounds of simulated hydrograph can be presented by using mean $\pm$ 2 $\times$ standard deviations.

5.4. Harr's point estimation method

By RPEM, 2^p model runs are required to estimate the statistical moments of the model output where p is the number of model parameters. Harr Milton (1989) proposed a modification that reduces the required model runs from 2^p to $2p$. HPEM (Harr Milton, 1989) can effectively mitigate the problems experienced with the RPEM for cases with numerous basic variables. Previous investigations summarized the method as follows (Yeh and Tung, 1993; Melching, 1995):

(a) Decompose the correlation matrix ρ of p stochastic input variables into an eigenvector matrix V and corresponding eigenvalue matrix as follows:

$$\rho = VLV^{\mathrm{T}} \quad (17)$$

where V is the eigenvector matrix (v_1, v_2,…, v_p) in which v_i are column vectors of eigenvectors, L a diagonal matrix of corresponding eigenvalues (λ_1, λ_2, …, λ_p); and the superscript T denotes the transpose of the matrix.

(b) Generate coordinates of the $2p$ intersecting points using

$$X_{i\pm} = X_m \pm p^{1/2} \begin{bmatrix} \sigma_1 & & & \\ & - & & 0 \\ & & - & \\ 0 & & & - \\ & & & \sigma_p \end{bmatrix} v_i \quad (18)$$

$i = 1, 2, \ldots, p$

(c) Calculate $Q_{i\pm} = H(X_{i\pm})$ and $Q^2_{i\pm} = H^2(X_{i\pm})$ for $i = 1, 2, \ldots, p$;
(d) Calculate the averaged model outputs for a given eigenvector $i = 1, 2, \ldots, p$ by using

$$Q_{mi} = (Q_{i+} + Q_{i-})/2 \text{ and } Q^2_{mi} = (Q^2_{i+} + Q^2_{i-})/2 \tag{19}$$

(e) Calculate the mean $E(Q)$ and variance $\mathrm{Var}(Q)$ of model output:

$$E[Q] = \frac{\left(\sum_{i=1}^{p} Q_{mi}\lambda_i\right)}{p} \tag{20}$$

$$E[Q^2] = \frac{\left(\sum_{i=1}^{p} Q^2_{mi}\lambda\right)}{p} \tag{21}$$

$$\mathrm{Var}(Q) = E[Q^2] - E^2[Q] \tag{22}$$

Herein, Eq. (17) was used as the correlation matrix ρ of the parameters (K_S, K_C, and CH) that were decomposed into an eigenvector V and corresponding eigenvalue matrix L as follows:

$$V = \begin{bmatrix} -0.9977 & 0.0293 & 0.0613 \\ 0.0226 & -0.7074 & 0.7064 \\ 0.0641 & 0.7062 & 0.7051 \end{bmatrix}$$

$$L = \begin{bmatrix} 1.0020 & 0 & 0 \\ 0 & 1.7006 & 0 \\ 0 & 0 & 0.2974 \end{bmatrix}$$

The eigenvalues, λ_1, λ_2, and λ_3 are 1.0020, 1.7006, and 0.2974, respectively.

Coordinates of the $2p$ ($p = 3$) intersecting points were generated via Eq. (18). Six sets of parameters were obtained as below:

(1) $\lambda_1 = 1.0020$

$K_{S1+} = 49.33 + \sqrt{3} \times 2.73 \times (-0.9977) = 44.61$

$K_{C1+} = 2.19 + \sqrt{3} \times 1.88 \times 0.0266 = 2.26$

$CH_{1+} = 0.96 + \sqrt{3} \times 0.79 \times 0.0641 = 1.05$

$K_{S1-} = 49.33 - \sqrt{3} \times 2.73 \times (-0.9977) = 54.05$

$K_{C1-} = 2.19 - \sqrt{3} \times 1.88 \times 0.0266 = 2.12$

$CH_{1-} = 0.96 - \sqrt{3} \times 0.79 \times 0.0641 = 0.87$

(2) $\lambda_2 = 1.7006$

$K_{S2+} = 49.33 + \sqrt{3} \times 2.73 \times (-0.0293) = 49.47$

$K_{C2+} = 2.19 + \sqrt{3} \times 1.88 \times (-0.7074) = -0.11 \approx 0$

$CH_{2+} = 0.96 + \sqrt{3} \times 0.79 \times (0.7062) = 1.93$

$K_{C2-} = 2.19 - \sqrt{3} \times 1.88 \times (-0.7074) = 4.49$

$K_{S2-} = 49.33 - \sqrt{3} \times 2.73 \times (-0.0293) = 49.19$

$CH_{2-} = 0.96 - \sqrt{3} \times 0.79 \times (0.7062) = -0.0063 \approx 0$

(3) $\lambda_3 = 0.2974$

$K_{S3+} = 49.33 + \sqrt{3} \times 2.73 \times 0.0613 = 49.62$

$K_{C3+} = 2.19 + \sqrt{3\times}1.88 \times 0.7064 = 4.49$

$CH_{3+} = 0.96 + \sqrt{3} \times 0.79 \times 0.7051 = 1.92$

$K_{S3-} = 49.33 - \sqrt{3} \times 2.73 \times 0.0613 = 49.04$

$K_{C3-} = 2.19 - \sqrt{3} \times 1.88 \times 0.7064 = -0.11 \approx 0$

$CH_{3-} = 0.96 - \sqrt{3} \times 0.79 \times 0.7051 = -0.0048 \approx 0$

By using these six sets of parameters (i.e. [K_{S1+}, K_{C1+}, CH_{1+}], [K_{S1-}, K_{C1-}, CH_{1-}], [K_{S2+}, K_{C2+}, CH_{2+}], [K_{S2-}, K_{C2-}, CH_{2-}], [K_{S3+}, K_{C3+}, CH_{3+}], and [K_{S3-}, K_{C3-}, CH_{3-}]) above in Eqs. (20) and (22) to determine the mean and variance of model output, the uncertainty bounds of simulated hydrograph can be obtained by indicating mean $\pm$ 2 $\times$ standard deviations at each time instant.

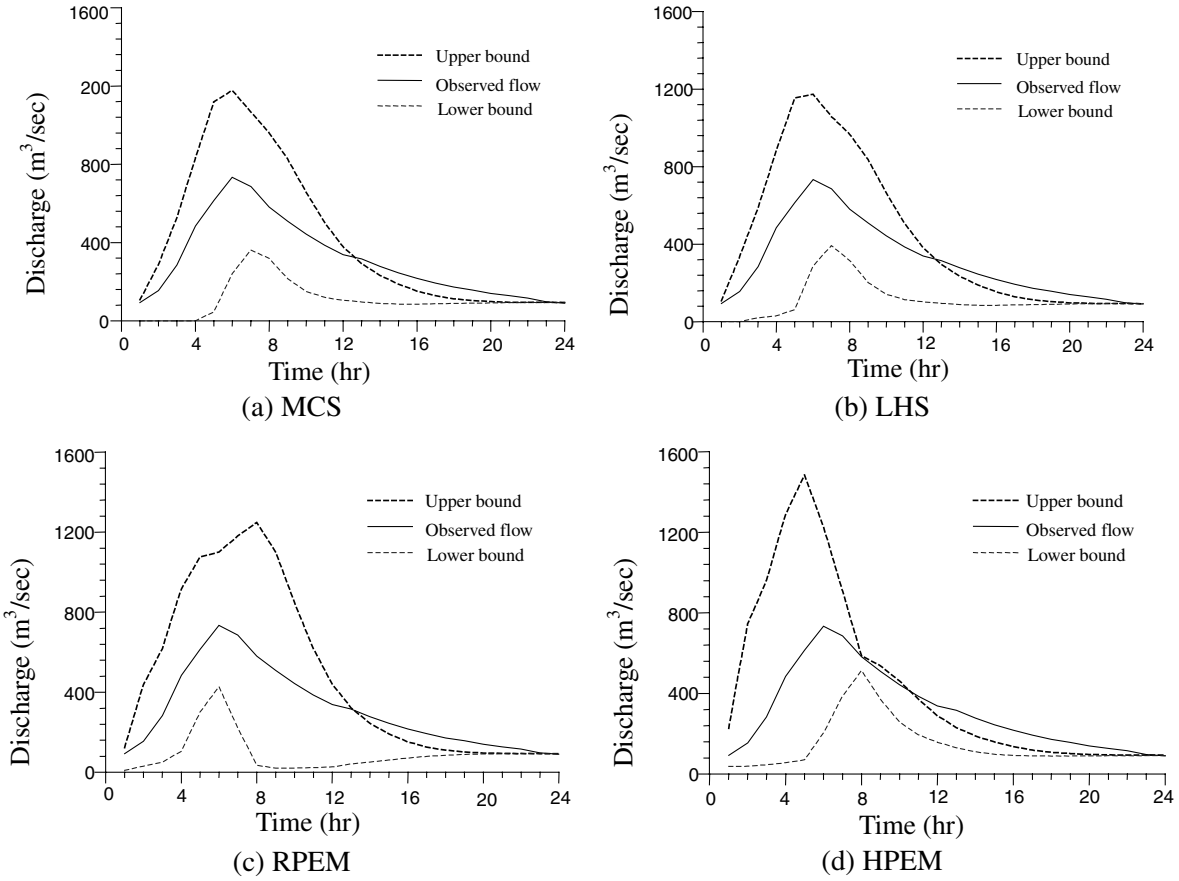

Fig. 8. The observed hydrographs and the uncertainty bounds (mean ± 2 × standard deviations) estimated by the MCS, LHS, RPEM, and HPEM for storm event VIII, respectively.

6. Results

This study selected three verification storm events excluded in calibration storm events to compare various methods of uncertainty analysis. Results obtained from the MCS for a large number of simulations (1000 runs) were assumed to be the standard results. Only one of three verification storm events (i.e. storm event VIII) is discussed here. Fig. 8 displays the uncertainty bounds of the hydrograph for storm event VIII estimated by the MCS, LHS, RPEM, and HPEM. Most of the observed hydrographs can be located in the uncertainty bounds except for the recession limb of the hydrograph. However, the uncertainty bounds estimated from various methods significantly differ from one another. Fig. 9 illustrates the mean and variance of the hydrograph estimated by various methods for storm event VIII in which only the LHS produces simulation results similar to the MCS. Additionally, the RPEM and HPEM have a markedly higher variance than the MCS. The average estimated hydrographs of the RPEM and HPEM also have a bias unlike the results of the MCS. Fig. 10 illustrates the peak discharge exceedance probability estimated by the MCS, LHS, RPEM, and HPEM for storm event VIII. The comparison also demonstrates that LHS could be a suitable replacement for MCS. Both the RPEM and HPEM have results that only roughly resemble those of the MCS. Apparently, the results of RPEM and HPEM are

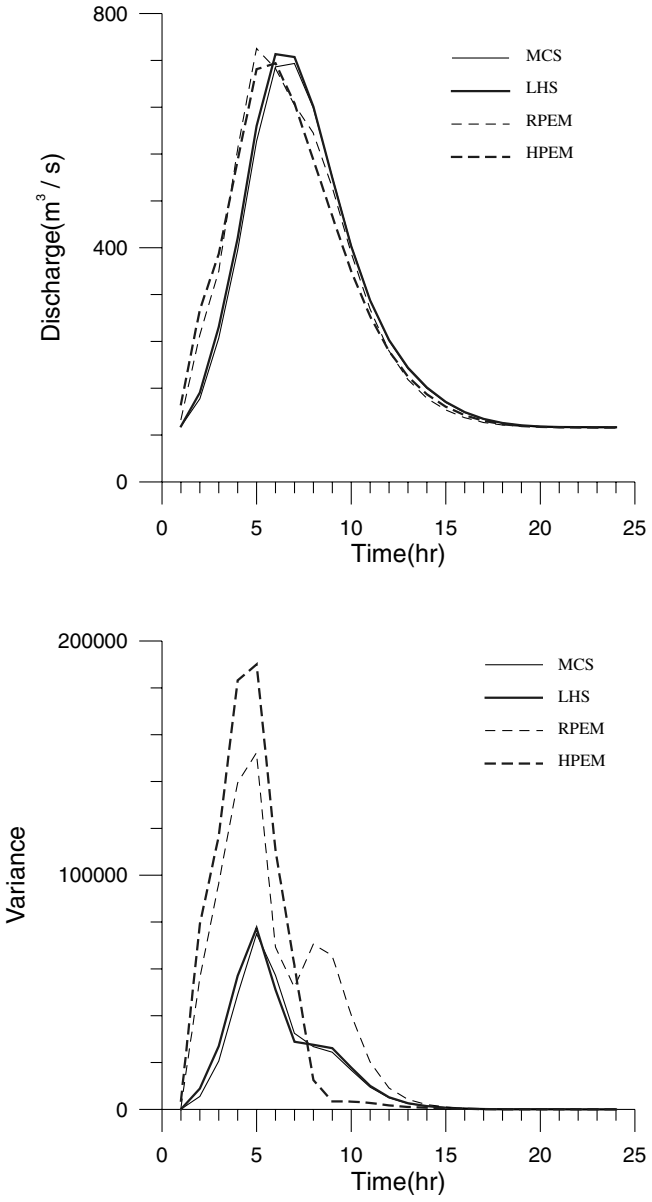

Fig. 9. The mean and variance of hydrographs estimated by various methods for storm event VIII.

biased with the results of MCS. The above results arise because the MCS and LHS can uniformly sample the parameters in their range. Moreover, the LHS can generate representative samples more efficiently than the MSC. Since samples of parameter generated by the RPEM and HPEM are associated with the number of model parameters in this study, the rainfall–runoff model has only three parameters leading to only eight and six sets of parameters being sampled by the RPEM and HPEM, respectively. The smaller sets of sampling parameters generated by the RPEM and HPEM have less representation than the MCS and LHS and reduce the accuracy of uncertainty estimation.

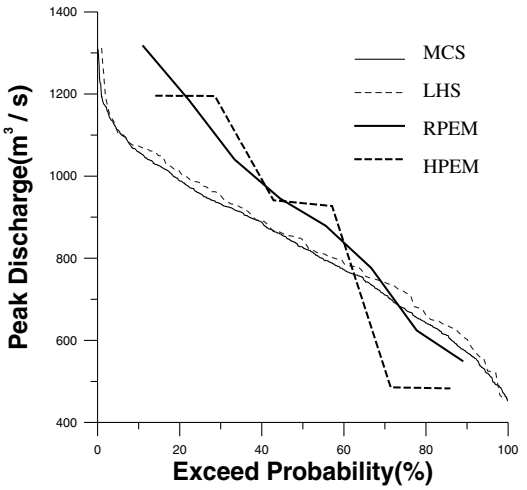

Fig. 10. Exceedance probability distributions of peak discharge estimated by various methods for storm event VIII.

7. Discussions

In this study, four methods (including MCS, LHS, RPEM, and HPEM) were applied to evaluate the effect on the model output of the parameter uncertainty. As the sampling mechanisms for various methods are different, various sample sizes are required to obtain the variance of model output. One thousand and 100 parameter sets were, respectively, found to be sufficient for MSC and LHS to analyze the uncertainty of model output and resulted in similar uncertainty estimates. It implied that the LHS method is more efficient than the MCS method to generate uncertainty in a hydrograph due to calibration parameters. The other two methods (RPEM and HPEM) require 2^p and $2p$ parameter sets, respectively, to estimate the statistical moments of model output where p is the number of model parameters. In our work with $p = 3$, the RPEM and HPEM methods only use eight and six parameter sets, respectively, far less than the parameter sets used by the MCS and LHS methods. Furthermore, the uncertainty of model output estimated by the RPEM and HPEM methods are very different from the result estimated by the MCS method. These results suggest to us that the two-point estimation methods (RPEM and HPEM) are not suitable for estimating the uncertainty of model output with a very small number of model parameters such as three calibration parameters in our study.

In Taiwan, hourly records for rainfall and runoff observations are not always available for all catchments. Observed runoff records are rarely scarce in some catchments. This phenomenon makes simulations of rainfall–runoff relationship more uncertain. Therefore, uncertainty analysis for a rainfall–runoff model is an essential issue for assessing uncertainty bounds of estimated hydrograph. Truly, it is difficult to determine the probable ranges of model parameters and their probability distributions by using such too few historical events for uncertainty analysis. Therefore, defining the probable range for each model parameter and hypothesizing its probability distribution are actually needed in this situation to hydrologists.

In our study, the range of each parameter for MCS and LHS methods is defined according to the calibrated results of six historical flood events. Due to the very small amount of historical events, the uniform distribution for each parameter is assumed and the probable range is decided by the calibrated results of model parameter. While sampling parameter sets by RPEM and HPEM methods is based on the parameter mean values and standard deviations that are calculated from the calibrated results of six historical flood events. Thus, the defined variation range of each parameter set is not strictly respected when the RPEM and HPEM methods are applied. The analyzed result also reveals that RPEM and HPEM methods produce parameter sets that cover a wider range than those considered for MCS and LHS methods. This result suggests that using RPEM and HPEM methods by using too few historical events may cause wider parameter ranges than those considered for MCS and LHS methods and the ranges of model parameters for RPEM and HPEM methods should be further checked for their plausibility.

In this study, it is found that odd values for some parameters may be produced when using RPEM and HPEM methods. Since these two methods try to use a relatively small amount of parameter sets to estimate the statistical moments of model output, this small amount of parameter sets has to include the probable parameter spaces representatively. Odd values of parameters may be considered as the limits of probable parameter spaces, but their plausibility should be checked before simulating the hydrographs. For instance, some sampling parameter sets by the HPEM method should be used with caution such as

the negative values of the parameters. If the negative value of a parameter has no physical meanings, the value of zero may be set equal to this parameter. In this study, when the HPEM method is applied, the negative values of the parameters, *K* and *CH* are set equal to zero for the sake of their physical meanings. A linear reservoir model with a constant *K* equal to zero makes storage equal to zero and means that inflow equals to outflow. And the parameter *CH* equal to zero means that the initial infiltration capacity is zero and the antecedent condition of catchment with great moisture, which are reasonable during the typhoon and heavy storm reason of Taiwan. Therefore, it is suggested and concluded that when using RPEM and HPEM methods, the produced parameter sets should be carefully checked for their plausibility.

8. Conclusions

The uncertainty of model output is a relevant concern for catchments with limited historical storm records and when the rainfall–runoff model is applied to storm events outside of the range of conditions for which the model has been successfully calibrated and verified.

This study investigated the uncertainty of model output caused by model calibration parameters by applying four methods of uncertainty analysis (MCS, LHS, RPEM, and HPEM). Six storm events were initially selected to calibrate the model. According to those analyzed results, the model can accurately simulate the historically observed hydrographs. The other three storm events were selected for uncertainty analysis. Those results affirm that the observed hydrographs of these three storm events can fall within the uncertainty bounds of mean $\pm 2 \times$ standard deviations estimated by the four methods except the recession limbs. However, the analytical results of these four methods differ significantly from one another. The results of the MCS for a large number of simulations were selected as the standard in the study. The investigation further confirmed that LHS could be used to replace the MCS because it produces results that are close to the MCS but using a relatively small number of simulations. In contrast, the results of the RPEM and HPEM differ significantly from the results of the MCS. This difference may have resulted from very small samples generated by RPEM and HPEM for uncertainty analysis due to the distributed rainfall–runoff model adopted in the work having only three model calibration parameters. These results also provide us a suggestion that the two-point estimation methods (RPEM and HPEM) are not suitable for estimating the uncertainty of model output with a very small number of model parameters and when using RPEM and HPEM methods, the produced parameter sets should be carefully checked for their plausibility.

Acknowledgements

The authors would like to thank the Council of Agriculture, Executive Yuan, Republic of China for financially supporting this research.

References

Abbott, M.B., Bathurst, J.C., Cung, J.A., O'Connell, P.E., Rasmussen, J., 1986. An introduction to the European hydrological system — systeme hydrologique European (SHE). 2: Structure of a physically based, distributed modelling system. Journal of Hydrology 87, 61–77.

Bates, B.C., Townley, L.R., 1988. Nonlinear, discrete flood event models. 3. Analysis of prediction uncertainty. Journal of Hydrology 99, 91–101.

Beven, K.J., O'Connell, P.E., 1982. On the role of physically based distributed modelling in hydrology, Report No.81, Institute of Hydrology, Wallingford, UK.

Beven, K.J., Kirkby, M.J., Schofield, N., Tagg, A.F., 1984. Testing a physically based flood forecasting model (Topmodel) for three UK catchments. Journal of Hydrology 69, 119–143.

Beven, K.J., 1989. Changing ideas in hydrology. The case of physically based models. Journal of Hydrology 105, 157–172.

Beven, K.J., Binley, A., 1992. The future of distributed models: model calibration and uncertainty prediction. Hydrological Processes 6, 279–298.

Binley, A.M., Beven, K.J., Calver, A., Watts, L.G., 1991. Changing responses in hydrology: assessing the uncertainty in physically based model predictions. Water Resources Research 27 (6), 1253–1261.

Brazil, L.E., Krajewski, W.F., 1987. Optimization of complex hydrologic models using random search methods, paper presented at Engineering Hydrology Conference, Hydraulic Division, American Society of Civil Engineers, Williamsburg, VA, August 3–7.

Diskin, M.H., Simpson, E.S., 1978. A quasi-linear spatial distribution cell model for the surface runoff system. Water Resources Bulletin 14, 903–918.

Diskin, M.H., Wyseure, G., Feyen, J., 1984. Application of a cell

model to the Bellebeek watershed. Nordic Hydrology 15, 25–38.

Duan, Q., Sorooshian, S., Gupta, V.K., 1992. Effective and efficient global optimization for conceptual rainfall–runoff models. Water Resources Research 28 (4), 1015–1031.

Duan, Q., Gupta, V.K., Sorooshian, S., 1993. A shuffled complex evolution approach for effective and efficient global minimization. Journal of Optimization Theory and Applications 76 (3), 501–521.

Edward, W.R., Woolhiser, D.A., Smith, R.E., 1977. A distributed kinematic model of upland watershed, Hydrology Paper No.93, Colorado State University.

Garen, D.C., Burges, S.J., 1981. Approximate error bounds for simulated hydrographs. Journal of the Hydraulics Division, ASCE 107 (HY11), 1519–1534.

Harr Milton, E., 1989. Probabilistic estimates for multivariate analysis. Applied Mathematical Modelling 13, 313–319.

Jayawardena, A.W., White, J.K., 1977. A finite element distributed catchment model (1): analysis basis. Journal of Hydrology 34, 269–286.

Jayawardena, A.W., White, J.K., 1979. A finite element distributed catchment model (2): application to real catchment. Journal of Hydrology 42, 231–249.

Jønch-Clausen, T., 1979. Systeme hydrological European (SHE): a short description, Report 1, Danish Hydraulics Institute, Horsholm, Denmark.

Knudsen, J., Thomsen, A., Refsgaard, J.C., 1986. WATBAL: a semi-distributed physically based hydrological modelling system. Nordic Hydrology 17, 347–362.

Laurenson, E.M., 1964. A catchment storage model for runoff routing. Journal of Hydrology 2, 141–163.

Lei, J., Schlling, W., 1993. Propagation of model uncertainty. In: Marsalek, J., Torno, H. (Eds.). Proceedings Sixth International Conference on Urban Storm Drainage, Niagara Falls, Canada. Seapoint Publishing, Victoria, BC, Canada, pp. 465–470.

Melching, C.S., 1992a. An improved first-order reliability approach for assessing uncertainties in hydrologic modeling. Journal of Hydrology 132, 157–177.

Melching, C.S., 1992b. A comparison of methods for estimating variance of water resources model predictions. In: Kuo, J.-T., Lin, G.-F. (Eds.). Stochastic Hydraulics '92, Proceedings Sixth International Association for Hydraulic Research Symposium on Stochastic Hydraulics, Taipei, Taiwan. Water Resources Publications, Littleton, CO, pp. 663–670.

Melching, C.S., 1995. Computer models of watershed hydrology. In: Vijay Singh, P. (Ed.). Reliability Estimation. Water Resources Publications, Littleton, CO, pp. 69–118.

Morris, E.M., 1980. Forecasting flood flows in grassy and forecasted catchments using a deterministic distributed mathematics model. IAHS Publication 129, 247–255.

Pederson, J.T., Peter, J.C., Helweq, O.J., 1980. Hydrographs by single linear reservoir model. ASCE 106 (HY5), 837–851.

Rosenblueth, E., 1975. Point estimates for probability moments. Proceedings of the National Academy of Sciences USA 72 (10), 3812–3814.

Rosenblueth, E., 1981. Two-point estimates in probabilities. Applied Mathematical Modelling 5, 329–335.

Ross, B.B., Contractor, D.N., Shanholtz, V.O., 1979. A finite element model of overland and channel flow for accessing the hydrologic impact of land use change. Journal of Hydrology 41, 11–30.

Sorooshian, S., Duan, Q., Gupta, V.K., 1993. Calibration of rainfall–runoff models: application of global optimization to the Sacramento soil moisture accounting model. Water Resources Research 29 (4), 1185–1194.

The Council of Agriculture, 1988. Soil survey maps, The Council of Agriculture, Executive Yuan, Taiwan, ROC.

Waren, V.J., Gary, L.L., John, W.K., 1989. Introduction to Hydrology. 3rd ed. Harper & Row/Bureau of Soil and Water Conservation, New York/Taiwan Province.

Yeh, K.C., Tung, Y.K., 1993. Uncertainty and sensitivity analysis of pit-migration model. Journal of Hydraulic Engineering 119 (2), 262–283.

Yu, P.S., Liu, K.W., 1992. A grid based watershed runoff model for Chyh-Lan Brook, CCNAA–AIT Joint Seminar on Prediction and Damage Mitigation of Meteorological Induced Natural Disasters, 21–22 May, Taipei, pp. 333–344.

Yu, P.S., Zheng, Y.C., 1997. A study on grid based distributed rainfall runoff model. Journal of Water Resource Management 11, 83–99.